Sympathetic laser cooling of graphene with Casimir-Polder forces

Sofia Ribeiro* and Hugo Terças
Instituto de Telecomunicações, Lisbon, Portugal
(Received 13 July 2016; published 24 October 2016)

We propose a scheme to actively cool the fundamental flexural (out-of-plane) mode of a graphene sheet via vacuum forces. Our setup consists of a cold-atom cloud placed close to a graphene sheet at distances of a few micrometers. The atoms couple to the graphene membrane via Casimir-Polder forces. By deriving a self-consistent set of equations governing the dynamics of the atomic gas and the flexural modes of the graphene, we show it is possible to cool graphene from room temperatures by actively (laser) cooling an atomic gas. By choosing the right set of experimental parameters we are able to cool a graphene sheet down to $\sim 60\ \mu$K.

DOI: 10.1103/PhysRevA.94.043420

I. INTRODUCTION

A lot of attention has been drawn in the last years to the development of quantum technologies with hybrid quantum systems whose elementary building blocks are of different nature [1]. The general trend is to combine well-characterized individual quantum systems, such as trapped ions [2,3], degenerate quantum gases [4], superfluid or superconducting Josephson junctions [5], quantum dots [6], and nanomechanical oscillators [7,8], with microwave guides, optical resonators, and fibers [9]. The most promising applications of such systems range from high-precision force and mass measurements to quantum computation [10–13]. Optomechanical setups have been particularly successful in that task, making it possible to cool down a mechanical system to its quantum ground state [14]. Radiation-pressure cooling of nano- or micromechanical cantilevers [15–19], vibrating microtoroids [20,21], and membranes [22] constitute important hallmarks in the field of optomechanics with important implications in quantum technologies.

With the advent of graphene and other two-dimensional materials, the zero-point cooling of macroscopic membranes becomes an imperative to the development of quantum technology based on suspended graphene. At low temperatures, the electrical resistivity in graphene is essentially hindered by the scattering between the electrons and the flexural (out-of-plane) phonons [23,24], which one could, in principle, cool down with the help of an optomechanical setup. However, given the broadband optical transmission of graphene (a graphene mirror is typically 98% transparent) [25], the coupling between the macroscopic mechanical motion and the photons is very unlikely, making radiation-pressure cooling totally ineffective [26]. As such, dilution refrigerators have been used in the attempt to approach the quantum limit. Recently, narrow-gap microwave-cavity cooling of graphene has brought the thermal motion of graphene down to $\sim$60 mK [27]. It is therefore natural to investigate suitable alternatives to radiation-pressure schemes by exploiting the advantage of interfaces with cold atoms. Recent results showed that sympathetic cooling with ultracold atoms enables us to reach ultralow temperatures in levitated optomechanical systems originally at room temperature when direct laser or evaporative cooling is not possible [28]. Also, it has been shown that heat transfer between two parallel layers of dipolar ultracold Fermi gases at different temperatures via dipolar couplings could be used as an effective cooling process [29].

There has been growing interest in exploring carbon nanotubes held at positive voltage to capture and ionize individual cold atoms [30,31] and also to explore the dispersion interactions between Bose-Einstein condensates and carbon nanotubes [32,33] and laser-controlled ultracold (Rydberg) atoms and graphene setups that may be used to create ripples on demand [34]. The dispersion forces arising from quantum fluctuations of the electromagnetic field between cold atoms and a carbon nanotube, commonly known as Casimir-Polder (CP) interaction [35], have been experimentally measured and pointed to as potentially useful for applications in quantum sensing and quantum information [33]. Immersing nanotubes in cold-atom clouds has also been suggested as a passive sympathetic cooling method [36]. In a recent study, the authors have theoretically examined the possibility of strong-coupling matter waves with a graphene sheet, paving the stage for non-destructive cold atom-graphene interfaces [37].

This article is organized as follows. In Sec. II, we introduce the Hamiltonian of the system. Using the Lamb-Dicke approximation, the adiabatic elimination of the electronic states, and linearization methods, we derive an effective master equation for the system. In Sec. III, we study the cooling process: not only do we derive the stationary state of the system, but also we calculate the cooling rate as a function of tunable experimental parameters. Finally, concluding remarks are provided in Sec. IV.

II. THEORETICAL MODEL

We propose a scheme to approach the quantum limit of the zero-point flexural motion of a graphene sheet by sympathetic laser-cooling via vacuum forces. Our setup consists of a laser-cooled two-dimensional cloud of cold atoms that is placed near the membrane (a few micrometers). At this distance, the atoms and the flexural modes couple as a consequence the CP interaction, allowing the exchange of excitations without destroying the atomic cloud [37]. By cooling the atomic motion with a far-detuned laser, we show that it is possible to effectively tailor the dissipation of the graphene membrane via vacuum fluctuations. Contrary to other optomechanical cooling protocols [27], our method offers the possibility of

*sofia.ribeiro@lx.it.pt

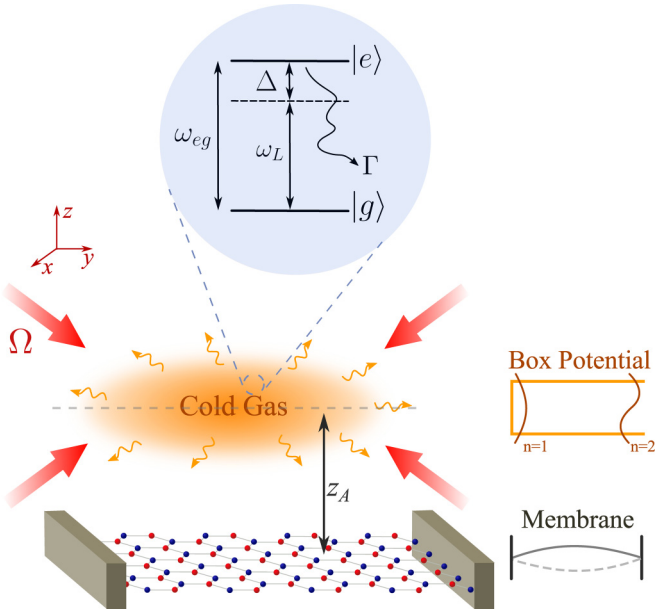

FIG. 1. Scheme of the experimental setup of a quantum gas at a distance z_A from a graphene sheet. The motion of the particles is coupled to the flexural modes of graphene via Casimir-Polder interactions. The cooling of the vibrational modes of the gas can be done with the help of the cooling laser with Rabi frequency Ω. For our calculations, we have chosen an atomic cloud of rubidium (^{87}Rb).

discarding dilution refrigerators and allows us to cool graphene to the quantum limit starting from room temperatures. Also, because it is nondestructive, it offers advantages with respect to Ref. [36] as it allows the *active* cooling of graphene zero-point motion to the quantum limit in steady state.

Our setup consists of a cold atomic gas confined in a two-dimensional box potential, in such a way that its transverse center-of-mass (phonon) modes are quantized (see Fig. 1), placed near a suspended graphene sheet (for our numerical calculations, we have chosen an atomic cloud of ^{87}Rb [38]). The phonons then couple to the flexural (out-of-plane) modes of a graphene sheet via vacuum CP forces, and the cooling laser drives D_2 ^{87}Rb transition. The aim of the laser cooling is to dissipate the atomic motion and, as a consequence, sympathetically cool down the flexural modes of the graphene sheet. In this paper, we will restrict our discussion to a single phonon mode coupled to a single flexural mode.

The Hamiltonian of the system in Fig. 1 can be written as

$$\hat{H} = \hat{H}_{\rm at} + \hat{H}_{\rm ph} + \hat{H}_{\rm flex} + \hat{H}_{\rm L} + \hat{H}_{\text{at-graph}}. \tag{1}$$

The first three terms are the energy of the electronic states of the atoms, their quantized vibrational modes, and the fundamental mode of the graphene sheet. Here, the cloud is composed of atoms with ground state $|g\rangle$, excited state $|e\rangle$, and transition frequency $\omega_{eg} = \omega_e - \omega_g$ (see Fig. 1); $\omega_{\rm ph}$ and ν are the center-of-mass (phonon) excitation in the atomic cloud and the flexural mode energies, respectively. Then, we can explicitly write

$$\hat{H}_{\rm at} = \hbar(\omega_e|e\rangle\langle e| + \omega_g|g\rangle\langle g|), \tag{2}$$

$$\hat{H}_{\rm ph} = \hbar\omega_{\rm ph}\hat{a}^\dagger\hat{a}, \tag{3}$$

$$\hat{H}_{\rm flex} = \hbar\nu\hat{f}^\dagger\hat{f}, \tag{4}$$

where $\hat{a}$ and $\hat{f}$ are the phonon and the flexural bosonic annihilation operators. The fourth term in Eq. (1) describes the coupling between the laser and the center-of-mass motion of the atoms [39], which can be written in the rotating wave approximation (RWA) as

$$\hat{H}_{\rm L} = \frac{\hbar}{2}\Omega[\sigma_-\hat{D}(i\eta)e^{i\omega_L t} + \text{H.c.}], \tag{5}$$

where ω_L is the laser frequency and $\Omega = \mathbf{d}_{ge}\cdot\boldsymbol{\epsilon}E_0/\hbar$ is the Rabi frequency of the transition $|g\rangle \to |e\rangle$ (with E_0 being the electric field amplitude, $\mathbf{d}_{ge}$ being the dipole operator, and $\boldsymbol{\epsilon}$ being the laser polarization). We have introduced the lowering and raising operators $\sigma_- = (\sigma_+)^\dagger = |g\rangle\langle e|$, and the displacement operator $\hat{D}(i\eta) \equiv e^{-i\eta(\hat{a}^\dagger+\hat{a})}$, with $\eta = \omega_{\rm rec}/\omega_{\rm ph}$ denoting the Lamb-Dicke parameter and $\omega_{\rm rec}$ denoting the recoil frequency. Taking advantage that the experimental parameters Ω, $\omega_{\rm ph}$, and $\Delta = \omega_{eg} - \omega_L$ are much smaller than the optical frequency, we can perform the atom-laser RWA Hamiltonian as [40]

$$\hat{H}_{\rm at} + \hat{H}_{\rm L} = \hbar\Delta\sigma_+\sigma_- + \frac{\hbar}{2}\Omega(\sigma_-\hat{D}(i\eta) + \text{H.c.}). \tag{6}$$

Finally, the last term in Eq. (1) is the Hamiltonian describing the interaction between the atoms and the graphene sheet that can be obtained by expanding the CP potential around the equilibrium position at first order in the displacement operator and averaging over the atomic density.

In general, the CP potential $U_{\rm CP}$ for planar surfaces has the form $U_{\rm CP}(z_A) = \frac{C_n}{z_A^n}$ (see Appendix A), with z_A being the vertical component of the atom-surface position $\mathbf{R}_A = (x_A, y_A, z_A)$. Details about its derivation can also be found in Refs. [41,42]. The potential for a very smooth surface can be obtained from the planar case by merely taking the local atom-surface distance

$$U(x,y,z) \simeq U^0_{\rm CP}(z_A) - u(\mathbf{r}_A)\frac{dU^0_{\rm CP}(z_A)}{dz_A}, \tag{7}$$

with $\mathbf{r}_A = (x_A, y_A)$. To obtain the interaction energy between atoms in the atomic gas and the corrugated membrane, one needs to sum the CP potential weighted by the atomic density and over the area of the membrane [36], i.e., $\hat{H}_{\text{at-graph}} = \int \frac{d\mathbf{R}}{\mathcal{V}} \int d\mathbf{R}'\, \hat{n}(\mathbf{R}')U(\mathbf{R}' - \mathbf{R})$. It is more convenient to transform it into the Fourier domain where it becomes a separable sum of products of atomic and graphene variables. This yields

$$\begin{aligned}\hat{H}_{\text{at-graph}} &= \sum_q \hat{a}^\dagger\hat{a}\, U^0_{\mathbf{q}} + i\sum_q \hat{a}^\dagger\hat{a}\,\mathbf{q}\cdot\hat{\mathbf{u}}_{\mathbf{q}}U^0_{\mathbf{q}} \\ &\equiv \hbar\sum_{\mathbf{q}} w_{\mathbf{q}}\hat{a}^\dagger\hat{a}(1 + i\mathbf{q}\cdot\hat{\mathbf{u}}_{\mathbf{q}}),\end{aligned} \tag{8}$$

where $U_{\mathbf{q}}$ is the Fourier transform of the potential $U^{|g\rangle}_{\rm CP}$, $w_{\mathbf{q}} \equiv U_{\mathbf{q}}/\hbar\sqrt{\mathcal{V}}$, and the phonon operator is expressed in the form $\hat{\mathbf{u}}_{\mathbf{q}} = \frac{1}{\sqrt{2}}\sum_\sigma \phi_{\mathbf{q},\sigma}(\mathbf{r})\mathbf{e}_\sigma(\hat{f}_\sigma + \hat{f}^\dagger_\sigma)$ with two polarizations $\sigma = (x,y)$, and the normalization condition $\langle\phi_{\mathbf{q}},\phi_{\mathbf{q}'}\rangle = \hbar/(M\nu)\delta_{\mathbf{q}\mathbf{q}'}$ is satisfied, where M is the membrane mass [37]. In our setup, we need to account for both electronic states $|g\rangle$ and $|e\rangle$ of the trapped particle, such that $\hat{a}^\dagger\hat{a} \to \hat{a}^\dagger\hat{a}|e\rangle\langle e| + \hat{a}^\dagger\hat{a}|g\rangle|g\rangle$. Moreover, we restrict our discussion to the fundamental mode $q_0 \equiv 2\pi/L$, with L representing the size of the graphene

sheet (here considered squared for definiteness; also see all the properties considered in Appendix B). After these considerations, the interaction Hamiltonian becomes

$$\hat{H}_{\text{at-graph}} = \hbar(\omega^{|e\rangle}|e\rangle\langle e| + \omega^{|g\rangle}|g\rangle\langle g|)\hat{a}^\dagger\hat{a}\hat{\mathcal{T}}. \tag{9}$$

Here, $\omega^{|i\rangle}$ is the Fourier transform of the CP potential of the electronic state $|i\rangle$, and $\hat{\mathcal{T}} \equiv 1 + i2q_0\sqrt{\hbar/(2m\nu)}(\hat{f} + \hat{f}^\dagger)$ is the translation operator.

A. Adiabatic elimination of the electronic states

In what follows, we assume that the detuning Δ is much larger than all other system parameters, $\Delta \gg \Omega, \omega_{\text{ph}}, \nu, \omega^{|i\rangle}, \Gamma$. Under such conditions, we are able to adiabatically eliminate the electronic states from the time evolution and obtain an effective master equation which reduces the evolution to the ground-state dynamics [43]. We assume the dynamics of the system to be Markovian, such that the time evolution density matrix ρ can be described by a master equation of Lindblad form,

$$\dot{\rho} = -\frac{i}{\hbar}[\hat{H},\rho] + \left[\hat{L}\rho\hat{L}^\dagger - \frac{1}{2}(\hat{L}^\dagger\hat{L}\rho + \rho\hat{L}^\dagger\hat{L})\right], \tag{10}$$

where $\hat{L}$ is the jump operator (to be specified below) accounting for the spontaneous decay of the electronic states. Following Ref. [43], by combining the perturbation theory of the density operator and adiabatic elimination of the excited state, we reduce the dynamics to an effective master equation involving only the ground-state manifold. The corresponding effective Hamiltonian and Lindblad operators are given by

$$\hat{H}_{\text{eff}} = -\frac{1}{2}\hat{V}_-\left[\hat{H}_{\text{NH}}^{-1} + \left(\hat{H}_{\text{NH}}^{-1}\right)^\dagger\right]\hat{V}_+ + H_{\text{g}}, \tag{11}$$

$$\hat{L}_{\text{eff}} = \hat{L}\hat{H}_{\text{NH}}^{-1}V_+, \tag{12}$$

where $\hat{V}_+$ ($\hat{V}_-$) is the perturbative excitation (deexcitation) operator of the system and $\hat{H}_g$ is the ground-state Hamiltonian. We have also introduced the non-Hermitian Hamiltonian of the quantum jump formalism as

$$\hat{H}_{\text{NH}} = \hat{H}_{\text{e}} - \frac{i}{2}\hat{L}^\dagger\hat{L}, \tag{13}$$

where $\hat{H}_{\text{e}}$ is the Hamiltonian in the excited manifold. The total Hamiltonian of the system can be explicitly written as

$$\hat{H} = \hat{H}_{\text{g}} + \hat{H}_{\text{e}}, \tag{14}$$

$$\hat{H}_{\text{g}} = \hbar\omega\hat{a}^\dagger\hat{a} + \hbar\nu\hat{f}^\dagger\hat{f} + \hbar\omega^{|g\rangle}|g\rangle\langle g|\hat{a}^\dagger\hat{a}\hat{\mathcal{T}}, \tag{15}$$

$$\hat{H}_e = \hbar\Delta|e\rangle\langle e| + \hbar\frac{\Omega}{2}[|g\rangle\langle e|\hat{D}(i\eta) + |e\rangle\langle g|\hat{D}^\dagger(i\eta)] + \hbar\omega^{|e\rangle}|e\rangle\langle e|\hat{a}^\dagger\hat{a}\hat{\mathcal{T}}, \tag{16}$$

and the raising and lowering can be written as

$$\hat{V}_+ = \hbar\frac{\Omega}{2}|e\rangle\langle g|\hat{D}^\dagger(i\eta), \quad \hat{V}_- = \hbar\frac{\Omega}{2}|g\rangle\langle e|\hat{D}(i\eta). \tag{17}$$

We further assume that the atoms are cooled enough to be in the Lamb-Dicke regime. In that case, we may write $\hat{D}^\dagger(i\eta) \simeq 1 + i\eta(\hat{a}^\dagger + \hat{a})$. Spontaneous emission from the excited to the ground state at a rate Γ is represented by the Lindblad operator $\hat{L} = \sqrt{\Gamma}|g\rangle\langle e|$. Consequently, the non-Hermitian Hamiltonian is found to be

$$\hat{H}_{\text{NH}} = \hbar\left(\Delta - i\frac{\Gamma}{2} + \omega^{|e\rangle}\hat{a}^\dagger\hat{a}\hat{\mathcal{T}}\right)|e\rangle\langle e| + \hbar\frac{\Omega}{2}[|g\rangle\langle e|\hat{D}(i\eta) + |e\rangle\langle g|\hat{D}^\dagger(i\eta)]. \tag{18}$$

Finally, by combining the approximations above, Eqs. (11) and (12), we obtain the effective Hamiltonian and Lindblad operators as

$$\hat{H}_{\text{eff}} = \hbar\omega\hat{a}^\dagger\hat{a} + \hbar\nu\hat{f}^\dagger\hat{f} + i\hbar g\,\hat{a}^\dagger\hat{a}(\hat{f}^\dagger + \hat{f}) + i\hbar\xi(\hat{a}^\dagger + \hat{a}), \tag{19}$$

$$\mathcal{L}_{\text{eff}}(\hat{O}) = \frac{\gamma}{2}\{2\hat{a}^\dagger\hat{O}\hat{a} - \hat{O}\hat{a}^\dagger\hat{a} - \hat{a}^\dagger\hat{a}\hat{O}\}. \tag{20}$$

Here, we have defined the reduced quantities $\omega = \omega_{\text{ph}} - \eta^2\hbar\Omega^2\Delta/(4\Delta^2 + \Gamma^2) + \omega^{|g\rangle}$, $\xi = \eta\hbar\Omega^2\Delta(4\Delta^2 + \Gamma^2)$, $g = 2q_0\sqrt{\hbar/(2m\nu)}n_0\omega^{|g\rangle}$, with n_0 being the atomic density, and $\gamma = \Gamma\eta^2\Omega^2/(\Gamma + 4\Delta^2)$, with Γ denoting the atomic spontaneous emission rate.

B. Linearization procedure

The effective Hamiltonian (19) is nonlinear in the phonon operator $\hat{a}$, which makes the handling of the equations of motion unpractical. Linearization of the Heisenberg-Langevin equations can be done in two ways [44]: the Hamiltonian linearization method, often used in optomechanics, and the equation linearization method, used in the semiclassical limit. Below we will perform the first. For that task, we make a displacement on the phonon operator around its average value α, $\hat{a} \to \alpha + \delta\hat{a}$, with $\langle\delta\hat{a}\rangle = 0$, such that the total phonon number is given by $|\alpha|^2 + \langle\delta\hat{a}^\dagger\delta\hat{a}\rangle$. Following [11], we start by considering the Hamiltonian without interactions $\hat{H} = \hbar\omega\hat{a}^\dagger\hat{a} + \hbar\nu\hat{f}^\dagger\hat{f} + i\hbar\xi(\hat{a}^\dagger + \hat{a})$. By applying a displacement operator $\hat{\mathcal{D}} = e^{\alpha^*\delta\hat{a} - \alpha\delta\hat{a}^\dagger}$ to a state vector $|\tilde{\psi}\rangle = \hat{\mathcal{D}}|\psi\rangle$, we can derive the transformed Hamiltonian $\tilde{H}$ by expanding the Schrödinger equation $i\hbar\partial_t|\tilde{\psi}\rangle = (i\hbar\dot{\hat{\mathcal{D}}} + \hat{\mathcal{D}}\hat{H}_{\text{eff}})|\psi\rangle$, which yields

$$\tilde{H} = i\hbar(\dot{\alpha}^*\delta\hat{a} - \dot{\alpha}\delta\hat{a}^\dagger) + \hat{\mathcal{D}}\hat{H}_{\text{eff}}\hat{\mathcal{D}}^\dagger. \tag{21}$$

Having in mind the property $\hat{\mathcal{D}}G(\hat{a},\hat{a}^\dagger)\hat{\mathcal{D}}^\dagger = G(\delta\hat{a} + \alpha, \delta\hat{a}^\dagger + \alpha^*)$, we find

$$\tilde{H} = \hbar\omega\delta\hat{a}^\dagger\delta\hat{a} + \hbar\omega|\alpha|^2 + \hbar\nu\hat{f}^\dagger\hat{f} - i\hbar\xi(\alpha^* - \alpha).$$

Similarly, we update the CP coupling and write

$$\hat{H}_{\text{at-graph}} = i\hbar g\delta\hat{a}^\dagger\delta\hat{a}(\hat{f}^\dagger + \hat{f}) + i\hbar g|\alpha|^2(\hat{f}^\dagger + \hat{f}) + i\hbar g(\alpha\delta\hat{a}^\dagger + \alpha^*\delta\hat{a})(\hat{f}^\dagger + \hat{f}), \tag{22}$$

where the first term corresponds to the three-wave mixing process and describes the intrinsic nonlinear process of our system; if we assume $\langle \delta\hat{a} \rangle \ll \alpha$, we can ignore this term and obtain the linearized Hamiltonian. The last term is the average CP coupling, with $g|\alpha|^2$ denoting the coupling strength. Finally, we obtain the linearized Hamiltonian and jump operators

$$\tilde{H} = \hbar\omega\delta\hat{a}^\dagger\delta\hat{a} + \hbar\omega|\alpha|^2 + \hbar\nu\hat{f}^\dagger\hat{f} + i\hbar g\,|\alpha|^2(\hat{f}^\dagger + \hat{f}) + i\hbar g\,(\delta\hat{a}^\dagger\alpha + \delta\hat{a}\alpha^*)(\hat{f}^\dagger + \hat{f}) - i\hbar\xi(\alpha^* - \alpha), \quad (23)$$

$$\tilde{\mathcal{L}}(\hat{O}) = \frac{\gamma}{2}\{2\delta\hat{a}^\dagger\hat{O}\delta\hat{a} - \hat{O}\delta\hat{a}^\dagger\delta\hat{a} - \delta\hat{a}^\dagger\delta\hat{a}\hat{O}\} + \frac{\gamma}{2}(\alpha[\delta\hat{a}^\dagger,\hat{O}] + \alpha^*[\hat{O},\delta\hat{a}]). \quad (24)$$

III. ANALYSIS OF THE COOLING PROCESS

We now solve the master equation to obtain the average number of phonons $n = \langle\hat{n}\rangle$ and flexurons $m = \langle\hat{f}^\dagger\hat{f}\rangle$ and the corresponding effective cooling rate $\gamma_{\rm eff}$. Making use of the property $\langle\dot{O}\rangle = \mathrm{Tr}\,[\hat{O}\dot{\rho}]$, Eq. (10) simply yields

$$\langle\dot{O}\rangle = -\frac{i}{\hbar}\langle[\hat{O},\hat{\tilde{H}}]\rangle + \frac{1}{2}\gamma\langle 2\hat{a}^\dagger\hat{O}\hat{a} - \hat{O}\hat{a}^\dagger\hat{a} - \hat{a}^\dagger\hat{a}\hat{O}\rangle + \frac{1}{2}\gamma\langle\alpha[\hat{a}^\dagger,\hat{O}] + \alpha^*[\hat{O},\hat{a}]\rangle. \quad (25)$$

Applying this equation to the mean flexural number $m(t)$, the mean phonon number $n(t)$, and the coherences $\hat{k}_1 = i(\hat{f}^\dagger + \hat{f})$, $\hat{k}_2 = \hat{f}^\dagger - \hat{f}$, $\hat{k}_3 = \alpha\hat{a}^\dagger + \alpha^*\hat{a}$, $\hat{k}_4 = i(\alpha\hat{a}^\dagger - \alpha^*\hat{a})$, $\hat{k}_5 = i(\alpha\hat{a}^\dagger + \alpha^*\hat{a})(\hat{f}^\dagger + \hat{f})$, $\hat{k}_6 = (\alpha\hat{a}^\dagger + \alpha^*\hat{a})(\hat{f}^\dagger - \hat{f})$, $\hat{k}_7 = (\alpha\hat{a}^\dagger - \alpha^*\hat{a})(\hat{f}^\dagger + \hat{f})$, $\hat{k}_8 = i(\alpha\hat{a}^\dagger - \alpha^*\hat{a})(\hat{f}^\dagger - \hat{f})$, $\hat{k}_9 = \hat{f}^{\dagger 2} + \hat{f}^2$, $\hat{k}_{10} = i(\hat{f}^{\dagger 2} - \hat{f}^2)$, $\hat{k}_{11} = (\alpha\hat{a}^\dagger)^2 + (\alpha^*\hat{a})^2$, and $\hat{k}_{12} = i[(\alpha\hat{a}^\dagger)^2 - (\alpha^*\hat{a})]^2$, we obtain a closed set of differential equations,

$$\begin{aligned}
\dot{n} &= g\hat{k}_7 - \gamma\hat{n} - \frac{\gamma}{2}\hat{k}_3,\\
\dot{m} &= g|\alpha|^2\hat{k}_2 + g\hat{k}_6,\\
\dot{k}_1 &= -\nu\hat{k}_2,\\
\dot{k}_2 &= \nu\hat{k}_1 - 2g|\alpha|^2 - 2g\hat{k}_3,\\
\dot{k}_3 &= \omega\hat{k}_4 - \gamma|\alpha|^2 - \frac{\gamma}{2}\hat{k}_3,\\
\dot{k}_4 &= -\omega\hat{k}_3 - 2g|\alpha|^2\hat{k}_1 - \frac{\gamma}{2}\hat{k}_4,\\
\dot{k}_5 &= -\nu\hat{k}_6 - \omega\hat{k}_7 - \frac{\gamma}{2}\hat{k}_5 - \gamma|\alpha|^2\hat{k}_1,\\
\dot{k}_6 &= \nu\hat{k}_5 - 2g|\alpha|^2\hat{k}_3 - 2g\hat{k}_{11} - 4g|\alpha|^2\hat{n} - 2g|\alpha|^2 + \omega\hat{k}_8 - \frac{\gamma}{2}\hat{k}_6 - \gamma|\alpha|^2\hat{k}_2,\\
\dot{k}_7 &= \nu\hat{k}_8 + \omega\hat{k}_5 - 2g|\alpha|^2\hat{k}_9 - 4g|\alpha|^2\hat{m} - 2g|\alpha|^2 - \frac{\gamma}{2}\hat{k}_7,\\
\dot{k}_8 &= -\nu\hat{k}_7 - 2g|\alpha|^2\hat{k}_4 - 2g\hat{k}_{12} - \omega\hat{k}_6 - 2g|\alpha|^2\hat{k}_{10} - \frac{\gamma}{2}\hat{k}_8,\\
\dot{k}_9 &= \nu\hat{k}_{10} - 2g|\alpha|^2\hat{k}_2 - 2g\hat{k}_6,\\
\dot{k}_{10} &= -\nu\hat{k}_9 - 2g|\alpha|^2\hat{k}_1 - 2g\hat{k}_5,\\
\dot{k}_{11} &= \omega\hat{k}_{12} - 2g|\alpha|^2\hat{k}_7 - \gamma\hat{k}_{11} - \gamma|\alpha|^2\hat{k}_3,\\
\dot{k}_{12} &= -\omega\hat{k}_{11} - 2g|\alpha|^2\hat{k}_5 - \gamma\hat{k}_{12} - \gamma|\alpha|^2\hat{k}_4.
\end{aligned}$$

In order to calculate the stationary flexural number $m_{\rm SS}$, we set all of the above equations to zero. This gives a set of 14 equations which can be readily solved to find $m_{\rm SS}$, $n_{\rm SS}$, and $k_i^{\rm SS}$. Defining the cubic frequencies $\mu^3 = \nu(\gamma^2 + 4\omega^2) + 16g^2\omega|\alpha|^2$ and $\lambda^3 = \nu(\gamma^2 + \omega^2) + 9g^2\omega|\alpha|^2$, we obtain

$$n_{\rm SS} = -\frac{-2\gamma^4\nu^2\omega|\alpha|^2 - 2\gamma^2\nu^2\omega^3|\alpha|^2 - 16\gamma^2g^4\omega|\alpha|^6 + 16\gamma^2g^4\omega|\alpha|^4 - 64g^4\omega^3|\alpha|^6}{2\omega\lambda^3\mu^3} - \frac{16g^4\omega^3|\alpha|^4 + \gamma^4g^2\nu|\alpha|^2 - 36\gamma^2g^2\nu\omega^2|\alpha|^4 + 5\gamma^2g^2\nu\omega^2|\alpha|^2 + 4g^2\nu\omega^4|\alpha|^2}{2\omega\lambda^3\mu^3}, \quad (26)$$

$$m_{\rm SS} = -\frac{(\gamma^2+\omega^2)(-48g^2\omega|\alpha|^2 - 3\gamma^2\nu + 4\nu^3 - 12\nu\omega^2)}{48\nu\omega\lambda^3} + \frac{3\omega - 2\nu}{6\omega} + \frac{|\alpha|^2(16\gamma^2g^2\omega|\alpha|^2 + 48g^2\nu^2\omega|\alpha|^2 - 32g^2\omega^3|\alpha|^2 + \gamma^4\nu + 4\gamma^2\nu^3 + 2\gamma^2\nu\omega^2 + 8\nu^3\omega^2 - 8\nu\omega^4)}{32\nu\omega\lambda^3} + \frac{(\gamma^2g|\alpha|^2 - 4g\omega^2|\alpha|^2)(-192g^4\omega^2|\alpha|^4 + 16g^2\nu^3\omega|\alpha|^2 - \gamma^4\nu^2 - 4\gamma^2\nu^4 + 18\gamma^2\nu^2\omega^2 + 8\nu^4\omega^2 - 8\nu^2\omega^4)}{32g\nu\omega\lambda^3\mu^3}. \quad (27)$$

We are especially interested in seeing how $m_{\rm SS}$ evolves with the parameters of the experiment g, Δ, and Ω, which we can tune by changing the atom-surface distance and during the cooling process. The evolution of the stationary-state number of the flexural modes is shown in Figs. 2(a) and 2(b); one can see that $m_{\rm SS}$ decreases by increasing the coupling strength g and Rabi frequency Ω. With an appropriate choice of Δ, Ω, and g, it is shown to be possible to have steady states with a low number of flexural modes ($\lesssim$10), which corresponds to temperatures below millikelvins. For the set

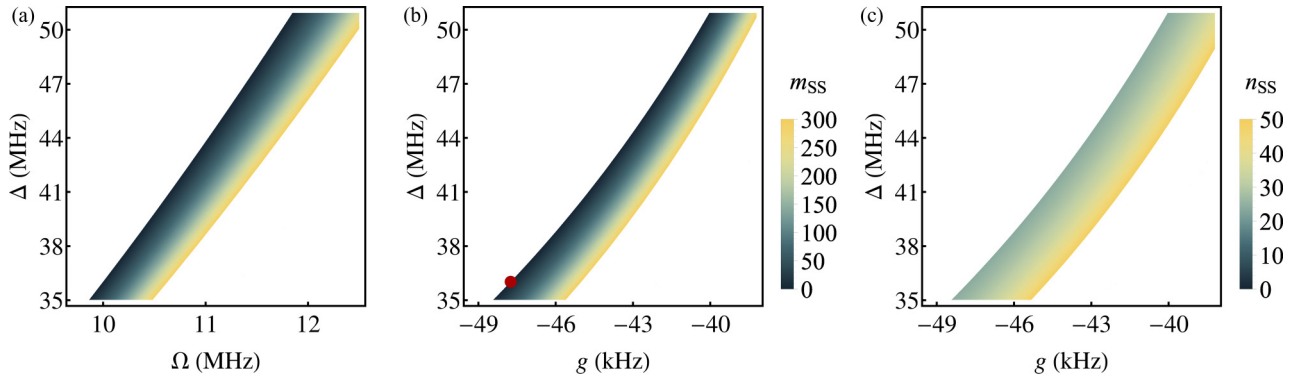

FIG. 2. Density plot of the stationary-state flexural mode number (a) and (b) m_{SS} and (c) n_{SS} for the parameters $\eta = 0.25$, $\Gamma = 6.07$ MHz, $\nu = 2.7$ MHz, $\omega_{ph} = 477$ Hz, where in (a) and (c) $\Omega = 10$ MHz and in (b) $g = -47.7$ kHz. The red point in (b) marks the coordinate $g = -47.7$ kHz and $\Delta = 36$ MHz, where $m_{SS} \sim 0.15$, for which the time evolution in Fig. 3 is calculated and corresponds to $n_{SS} \approx [\exp[\hbar\omega_{ph}/(k_B T_{atoms})] - 1]^{-1} \sim 24$, for which the temperature is $T_{atoms} = 560$ nK.

of parameters chosen, $\eta = 0.25$, $\Gamma = 6.07$ MHz, $\nu = 2.7$ MHz, $\Omega = 10$ MHz, $\omega_{ph} = 477$ Hz, $g = -47.7$ kHz, and $\Delta = 36$ MHz [corresponding to the red point depicted in Fig. 2(b)], we obtain $m_{SS} \sim 0.15$, which corresponds to a temperature of $T_{graph} \simeq 60$ μK. Correspondingly, the atomic motion is limited to $n_{SS} \sim 24$ [see Fig. 2(c)], for which we find $T_{atoms} = 560$ nK. This is consistent with the Lamb-Dicke approximation for a two-dimensional gas confined in a box potential of frequency ω_z of the order of a few kilohertz [45,46]. Although the atoms and the graphene sheet dynamics reach the steady state, we remark that the system is not in thermal equilibrium. Therefore, the temperatures T_{atoms} and T_{graph} are merely effective and not necessarily equal. Indeed, the effective temperatures after the cooling process are obtained by fitting the corresponding steady-state occupations n_{SS} and m_{SS} with Bose-Einstein statistics.

For comparison, let us look at conventional cryogenic refrigeration processes that can be used to cool a vibrational mode of a mechanical resonator to its quantum ground state. In Ref. [47], this is done by using a microwave-frequency mechanical oscillator coupled to a quantum bit. In this cooling process, the maximum number of phonons obtained in the relevant mechanical mode is $m_{max} < 0.07$. Laser-cooling techniques can also provide a general and flexible method of preparing macroscopic objects in their motional ground state where the strong coupling allows for the coherent exchange of photons and mechanical flexural modes; for these techniques, it is possible to obtain $m = 0.3$–0.8, [7,48,49]. Laser techniques can also be used to cool a vibrational mode in graphene or to power a graphene-based tunable frequency oscillator [26]. In Ref. [27], it is shown to be possible to cool down graphene to 60 mK, corresponding to an occupation number of 50, nearly three orders of magnitude lower than what has been recorded with different techniques. For the parameters chosen, our result lies at least two orders of magnitude below this experimental record, but other parameters may lead to even lower occupation numbers.

A. Cooling dynamics

For an analytical estimate of the effective cooling rate γ_{eff}, we use the fact that the mean flexural mode number m evolves on a relatively slow time scale compared to that of all other variables, the dynamics of which can be adiabatically eliminated by setting $\langle \dot{k}_i \rangle = 0$ and $\langle \dot{n} \rangle = 0$. We find the expressions $\hat{k}_2 = 0$ and $\hat{k}_6 = \mathcal{F}(m(t))$; that is, $\hat{k}_6$ is a function of the mean flexural number. Substituting these in $\dot{\hat{m}}(t) = g|\alpha|^2\hat{k}_2 + g\hat{k}_6$, we obtain an expression where $\dot{\hat{m}}(t) = g\mathcal{F}(m(t))$. Solving this equation yields finding $m(t) = ae^{\gamma_{eff}t} + m_{SS}$ with m_{SS} given by Eq. (27),

$$
\begin{aligned}
a = \Bigg(& \frac{1}{\nu\omega}\{32g^4\omega^2|\alpha|^8[\gamma^2 + 4(3\nu^2 + \omega^2)]. \\
& + 16g^2\omega|\alpha|^6[\gamma^4\nu + 2\gamma^2(8g^2\omega + 2\nu^3 + \nu\omega^2) \\
& - 8\omega(g^2\{-6\nu^2 + 9\nu[2m(0) + 1]\omega - 2\omega^2\} - \nu^3\omega \\
& + \nu\omega^3)] + |\alpha|^2\nu^2(\gamma^2 + \omega^2)(\gamma^2 + 4\omega^2)(\gamma^2 + 4\{\nu^2 - 2\nu \\
& \times [2m(0) + 1]\omega + \omega^2\})2\nu\omega|\alpha|^4[\gamma^2\nu\omega(7\gamma^2 + 12\nu^2 \\
& - 20\omega^2) + 4g^2(4\gamma^4 + \gamma^2\{14\nu^2 - 25[2m(0) + 1]\nu\omega \\
& + 20\omega^2\} + 4\omega^2\{8\nu^2 - 13[2m(0) + 1]\nu\omega + 4\omega^2\})]\}\Bigg) \\
& \div \{16[g^2\omega|\alpha|^4(25\gamma^2\nu + 144|\alpha|^2g^2\omega + 52\nu\omega^2) \\
& + |\alpha|^2\nu^2(\gamma^2 + \omega^2)(\gamma^2 + 4\omega^2)]\},
\end{aligned}
\tag{28}
$$

where $m(0) = [\exp(\frac{\hbar\nu}{k_B T_{graph}}) - 1]^{-1}$ is the occupation number calculated at $t = 0$ and initial temperature T_{graph}, and the cooling rate given by

$$
\begin{aligned}
\gamma_{eff} = & \{64\gamma g^2\lambda^3\nu^2\omega|\alpha|^2\} \\
& \div (32g^2\omega|\alpha|^2\{8g^2\omega|\alpha|^2(\gamma^2 - 3\nu^2 + \omega^2) \\
& + \nu[\gamma^4 + 5\omega^2(\gamma^2 - 2\nu^2) - \gamma^2\nu^2 + 4\nu^4 + 4\omega^4]\} \\
& + \nu^2(\gamma^2 + \omega^2)[\gamma^4 + 8\gamma^2(\nu^2 + \omega^2) + 16(\nu^2 - \omega^2)^2]).
\end{aligned}
\tag{29}
$$

In the parameter regions for which the cooling is stable (i.e., for which the rate γ_{eff} is positive, corresponding to the shaded regions in Fig. 2), cooling is possible independent of the initial graphene temperature. Figure 3 compares the sympathetic graphene laser-cooling dynamics for different initial occupation numbers $m(0)$. The exponential reduction of the occupation flexural number only slows downs until

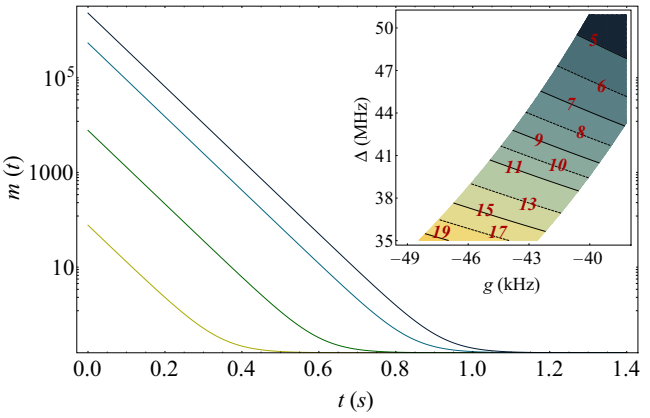

FIG. 3. Logarithmic plot of the time evolution of the mean flexural mode number m for the same parameters as in Fig. 2(b), but with $g = -47.7$ kHz and $\Delta = 36$ MHz. The different lines represent different starting temperatures, from bottom to top, $T = 0.01, 1, 70, 300$ K. For these parameter the $m_{SS} = 0.15$, which corresponds to a final temperature of $T_{graph} = 60\,\mu$K. The inset shows a contour plot of γ_{eff} as a function of g and Δ for the same parameters as in Fig. 2(b).

m reaches its stationary state value and $\gamma_{eff} \approx 2.87$ Hz. Even starting from room temperature, the stationary state is reached within an experimentally reasonable time scale ($\tau_{eff} \simeq 0.35$ s). In a recent work [29], sympathetic cooling via dipolar interactions between particles with permanent electrical dipoles was proposed (please note that in our proposal the interaction is between well-separated neutral objects with no permanent dipoles). Although we cannot quantitatively compare the steady-state particle number results, the time evolution to reach thermal equilibrium between the dipolar gases separated by a few micrometers is less than tens of milliseconds. For the most widely used cooling scheme, sideband cooling, the cooling rate γ_{cool} and, conversely, the time required to approach the ground state of a mechanical resonator are inherently limited by the mechanical frequency, $\gamma_{cool} < \nu$. However, techniques such as the pulsed-cooling method for mechanical oscillators are expected to surpass this intrinsic limit [11].

B. Effects of temperature and the g coupling parameter

It is important to keep in mind the experimental limitations to the cooling protocol. First, due to the difference in temperatures between the two media, our calculations of the CP potential would, in principle, require out-of-equilibrium corrections. For the general case, $T_{atoms} \neq T_{graph}$, the nonequilibrium CP energy can be written as the sum of two contributions [50,51],

$$E_{th}^{neq}(T_{atoms}, T_{graph}, z_A) = E_{th}^{eq}(z_A) + E^{neq}(T_{atoms}, T_{graph}, z_A).$$

Accounting for out-of-equilibrium corrections could lead to different distance power laws or a change in the nature of the CP force from attractive to repulsive [51]. Having those eventual limitations in mind, we have fixed the value $g = -47.7$ kHz to illustrate and better compare the cooling dynamics in Fig. 3. The coupling strength, defined by

$$g = 2q_0\sqrt{\frac{\hbar}{2m\nu}}n_0\omega^{|g\rangle},$$

can be experimentally adjusted by tuning the atom-surface distance, temperature, and atomic density.

There are two different limits for the CP interaction [35]. In the retarded limit, when the atom-surface distance z_A is large compared to the effective transition wavelength, $z_A \gg c/\omega_{eg}$, the CP potential is given by $U_{CP}^{|g\rangle} = C_4/z_A^4$, where one finds $C_4 = 14.26$ Hz μm^4 for graphene interfacing with ^{87}Rb in the ground state at $T = 0$. Moreover,

$$\hbar\omega^{|g\rangle} = \pi C_4 q_0 \frac{K_1(q_0 z_A)}{z_A}$$

is the Fourier transform of the CP potential $U_{CP}^{|g\rangle}$, with $K_1(x)$ denoting the modified Bessel function of the second kind [37]. In the nonretarded limit, $z_A \ll c/\omega_{eg}$, $U_{CP}^{|g\rangle} = C_3/z_A^3$, one finds $C_3 = 215.65$ Hz μm^3, and the Fourier transform becomes

$$\hbar\omega^{|gt\rangle} = 2\pi C_3 \frac{e^{-q_0 z_A}}{z_A}.$$

For the numerical calculations, we tried to choose parameters close to real experimental setups; as such, the coupling chosen, $g = -47.7$ kHz, can be obtained at $z_A \approx 0.2\,\mu$m, considering a density $n_0 \approx 10^{18}$ atoms/cm^3 and a squared graphene with size $L_{graph} = 5\,\mu$m and $\nu = 2.7$ MHz. The same order of magnitude values could be obtained for other experimental situations (even if the scaling law is different). However, we would like to remark that our analysis is still valid for smaller values of g (up to one order of magnitude smaller), leading to cooling times of the order of tens of seconds, still compatible with state-of-the-art trap lifetimes.

Also, at higher temperatures, it may happen that we would need to include the effect of excited mechanical modes. The zero-mode cooling would therefore depend upon the difference between two (or more) consecutive modes. When this difference is larger than the effective damping of the excited mode, we expect the cooling process not to be affected [52]. However, for the sake of simplicity, we can assume that a potential experiment with cold atoms could be performed at sufficiently low temperatures for both graphene and the atomic cloud for thermal excitations to only play a secondary role; thus, such corrections are negligible for the atomic temperatures, and deviations from the zero-temperature result are not in order. Second, blackbody radiation effects could also lead to additional heating of the atoms [53]. In a separate study, we have shown that this effect is not relevant for distances of a few micrometers [37].

C. Experimental limitations

We would also like to make a few comments regarding the experimental realization of such a proposal setup that will require placing and controlling an atomic gas very close to a surface. Controlling the atoms so close to a surface is an ambitious task since the CP forces are comparable with the typical trapping forces for cold atoms. Using magnetic traps, it has been shown that it is possible to stably trap atomic

clouds at distances of 500 nm [13,54]. Other techniques, such as using optical dipole traps based on evanescent waves, allows one to reach distances of 215 nm [55,56] or to achieve distances of 100 nm by using tightly focused optical tweezers [57]. Finally, the laser light used to cool (and eventually trap) the atoms could induce some additional heating to graphene. Fortunately, two-dimensional, pancakelike clouds of atoms of thickness $L_z \sim 0.3$–$0.6\,\mu$m are experimentally accessible [46], therefore minimizing physical contact between the laser and the membrane.

IV. CONCLUSION

In conclusion, we have shown that is possible, via the CP interactions between an atomic gas and a graphene sheet, to cool the mechanical out-of-plane vibrations by laser cooling the phonon excitations in the quantum gas. Sympathetic laser cooling via the vacuum forces is shown to reach temperatures of $\sim$60 μK, about 100 times cooler than the temperature reached by the usual optomechanical methods ($\sim$60 mK). Cooling a membrane to its ground state creates a path to new hybrid systems where the motion of mechanical resonators can be coupled with other quantum systems. One can imagine that the membrane could act as a transducer providing coupling between, for instance, photons or spins. Such transducers could play an important role in quantum networks. For the condensed-matter physics point of view, the interest lies in cooling the mechanical modes of graphene and, consequently, controlling the transport properties. Since the mobility of carriers in graphene membranes is extremely sensitive to temperature, flexural phonons are the leading scattering mechanism for temperatures higher than few kelvin; by cooling the mechanical modes of a graphene membrane it would then be possible to decrease the resistivity of the membrane.

ACKNOWLEDGMENTS

The authors acknowledge the Security of Quantum Information Group for the hospitality and for providing the working conditions. The authors are thankful for the support from Fundação para a Ciência e a Tecnologia (Portugal), namely, through the projects UID/EEA/50008/2013 IT/QuSim and through scholarship SFRH/BPD/110059/2015. Fruitful discussions with J. D. Rodrigues are also acknowledged.

APPENDIX A: CASIMIR-POLDER PHYSICS

For planar structures, the CP potential of an atom in the ground state at a distance z_A away from the macroscopic body with permittivity $\varepsilon(\omega)$ can be written as [35]

$$U_{\rm CP}^{|g\rangle}(z_A) = \frac{\hbar\mu_0}{8\pi^2}\int_0^\infty d\xi\,\xi^2\alpha_{at}(i\xi)\int_0^\infty dk_\parallel \frac{e^{-2k_\parallel\gamma_{0z}z_A}}{\gamma_{0z}} \times\left[\mathrm{R_{TE}}+\mathrm{R_{TM}}\left(1-\frac{2k_\parallel^2\gamma_{0z}^2c^2}{\xi^2}\right)\right], \tag{A1}$$

and for an atom in an energy eigenstate $|n\rangle$ it can be written as

$$U_{\rm CP}^{|n\rangle}(z_A) = \frac{\hbar\mu_0}{8\pi^2}\int_0^\infty d\xi\,\xi^2\alpha_n(i\xi)\int_0^\infty dk_\parallel \frac{e^{-2k_\parallel\gamma_{0z}z_A}}{\gamma_{0z}} \times\left[\mathrm{R_{TE}}+\mathrm{R_{TM}}\left(1-\frac{2k_\parallel^2\gamma_{0z}^2c^2}{\xi^2}\right)\right] + \frac{\mu_0}{4\pi}\sum_{k\neq n}\omega_{nk}^2\mathbf{d}_{nk}\cdot\mathbf{d}_{kn}\int_0^\infty d\kappa_{0z}e^{-2\kappa_{0z}z_A} \times\mathrm{Re}\left[\mathrm{R_{TE}}+\mathrm{R_{TM}}\left(1+\frac{2\kappa_{0z}^2c^2}{\omega^2}\right)\right], \tag{A2}$$

where $\gamma_{iz}=\sqrt{1+\varepsilon_i(i\xi)\xi^2/(c^2k_\parallel^2)}$, $\kappa_{0z}=\sqrt{k_\parallel^2+\omega^2/c^2}$, ω_{ij} ($\mathbf{d}_{ij}$) is the transition frequency (dipole moment), and $\alpha_n(\omega)$ is the atomic polarizability defined by

$$\alpha_n(\omega)=\lim_{\varepsilon\to0}\frac{2}{\hbar}\sum_{k\neq n}\frac{\omega_{kn}\mathbf{d}_{nk}\cdot\mathbf{d}_{kn}}{\omega_{kn}^2-\omega^2-i\omega\varepsilon}\,. \tag{A3}$$

The first term in Eq. (A2) describes the nonresonant part of the CP potential, recognizable by the integration along the imaginary frequency axis, $\omega=i\xi$, whereas the second term is related to resonant photon exchange between the atom and the graphene sheet. Equations (A1) and (A2) are strictly valid only at zero temperature. We are assuming potential experimental setups that could be performed at sufficiently low temperatures for thermal excitations to only play a subordinant role; in addition, the distance between the atoms and the graphene sheet is assumed to be much smaller than the thermal wavelength $\lambda_T=hc/(k_BT)$. In situations in which either assumption fails to hold, a replacement of the frequency integral by a Matsubara sum,

$$\frac{\hbar}{\pi}\int_0^\infty d\xi\; f(i\xi)\mapsto 2k_BT\sum_{n=0}^{\infty}\left(1-\frac{1}{2}\delta_{0n}\right)f(i\xi_n)\,, \tag{A4}$$

with Matsubara frequencies $\xi_n=2\pi k_BTn/\hbar$ [58], has to be employed. Thermal corrections become important only for $k_BT\gtrsim\Delta$, where Δ is the gap parameter of quasiparticle excitations [59]. At finite temperature, the potential is well approximated by inserting the temperature-dependent reflection coefficients in the lowest term in the Matsubara sum ($j=0$) while keeping the zero-temperature coefficients for all higher Matsubara terms [60,61].

Due to graphene's unique electronic structure, a full calculation of its electromagnetic reflection coefficients is, in fact, possible from first principles. Using the Dirac model for the description of the dynamics of quasiparticles in graphene at zero temperature in external electromagnetic fields, one can, by imposing appropriate boundary conditions to the fields, find the reflection coefficients for given values of the mass gap m and chemical potential μ. For simplicity, we will set $m=\mu=0$ (perfect Dirac cone) for which the difference between this approximation for suspended graphene samples ($m,\mu\sim0.01$ eV) is less than 1% [62]. One then arrives at the reflection coefficients of a free-standing graphene sheet in

vacuum as

$$R_{\mathrm{TM}} = \frac{4\pi\alpha\sqrt{k_0^2 + k_\parallel^2}}{4\pi\alpha\sqrt{k_0^2 + k_\parallel^2} + 8\sqrt{k_0^2 + \tilde{v}^2 k_\parallel^2}}, \tag{A5}$$

$$R_{\mathrm{TE}} = -\frac{4\pi\alpha\sqrt{k_0^2 + \tilde{v}^2 k_\parallel^2}}{4\pi\alpha\sqrt{k_0^2 + \tilde{v}^2 k_\parallel^2} + 8\sqrt{k_0^2 + k_\parallel^2}}, \tag{A6}$$

where we define $k_0^2 = \xi^2/c^2$ and $\tilde{v} = (300)^{-1}$ and $\alpha = 1/137$ is the fine-structure constant.

APPENDIX B: GRAPHENE PROPERTIES

It is well known that a free-floating graphene sheet will always crumple at room temperature; hence, to perform our setup there is a need to support the graphene sheet on a trench. Measurements on layered graphene sheets with a thickness between 2 and 8 nm have provided spring constants that scale as expected with the dimensions of the suspended section and range from 1 to 5 N/m [63]. Other experiments studied the fundamental resonant frequencies from electromechanical resonators made of graphene sheets [64]. For mechanical resonators under tension T, the fundamental resonance mode f_0 is given by

$$f_0 = 2\pi\left\{\left[A\sqrt{\frac{E}{\rho}}\frac{t}{L^2}\right]^2 + A^2 0.57\frac{T}{\rho L^2 w t}\right\}^{1/2}, \tag{B1}$$

where E is Young's modulus; ρ is the mass density; t, w, L are the thickness, width, and length of the suspended graphene sheet; and A is a clamping coefficient (A is equal to 1.03 for doubly clamped beams and 0.162 for cantilevers). We assume a doubly clamped sheet with a finite value for the tension $T = 1$ nN. Tension between graphene and trenches depends on the fabrication technique, but the interaction with the substrate is generally quite difficult to control [64]. For our purposes, we have used the known values for bulk graphite $\rho = 2200\,\mathrm{kg/m^3}$ and $E = 1.0$ TPa for a doubly clamped graphene sheet with $t = 0.3$ nm, $L = 5\ \mu$m, and $w = 5\ \mu$m.

[1] M. Saffman, T. G. Walker, and K. Mølmer, Rev. Mod. Phys. **82**, 2313 (2010).
[2] L. Tian and P. Zoller, Phys. Rev. Lett. **93**, 266403 (2004).
[3] S. Schmid, A. Härter, and J. H. Denschlag, Phys. Rev. Lett. **105**, 133202 (2010).
[4] *Quantum Gases: Finite Temperature and Non-equilibrium Dynamics*, edited by S. Gardiner, N. Proukakis, and M. Davis (Imperial College Press, London, 2013).
[5] M. Grupp, W. P. Schleich, E. Goldobin, D. Koelle, R. Kleiner, and R. Walser, Phys. Rev. A **87**, 021602 (2013), and references therein.
[6] A. Recati, P. O. Fedichev, W. Zwerger, J. von Delft, and P. Zoller, Phys. Rev. Lett. **94**, 040404 (2005).
[7] J. Chan, T. P. Mayer Alegre, A. H. Safavi-Naeini, J. T. Hill, A. Krause, S. Groeblacher, M. Aspelmeyer, and O. Painter, Nature (London) **478**, 89 (2011).
[8] M. Poot and H. S. J. van der Zant, Phys. Rep. **511**, 273 (2012).
[9] I. B. Mekhov and H. Ritsch, J. Phys. B **45**, 102001 (2012).
[10] E. Gavartin, P. Verlot, and T. J. Kippenberg, Nat. Nanotechnol. **7**, 509 (2012).
[11] S. Machnes, J. Cerrillo, M. Aspelmeyer, W. Wieczorek, M. B. Plenio, and A. Retzker, Phys. Rev. Lett. **108**, 153601 (2012).
[12] B. H. Schneider, S. Etaki, H. S. J. van der Zant, and G. A. Steele, Sci. Rep. **2**, 599 (2012).
[13] D. Hunger, S. Camerer, T. W. Hänsch, D. König, J. P. Kotthaus, J. Reichel, and P. Treutlein, Phys. Rev. Lett. **104**, 143002 (2010).
[14] F. Marquardt and S. M. Girvin, Physics **2**, 40 (2009).
[15] C. Höhberger-Metzger and K. Karrai, Nature (London) **432**, 1002 (2004).
[16] S. Gigan, H. R. Bohm, M. Paternostro, F. Blaser, G. Langer, J. B. Hertzberg, K. C. Schwab, D. Bauerle, M. Aspelmeyer, and A. Zeilinger, Nature (London) **444**, 67 (2006).
[17] O. Arcizet, P. F. Cohadon, T. Briant, M. Pinard, and A. Heidmann, Nature (London) **444**, 71 (2006).
[18] D. Kleckner and D. Bouwmeester, Nature (London) **444**, 75 (2006).
[19] C. Regal, J. Teufel, and K. Lehnert, Nat. Phys. **4**, 555 (2008).
[20] T. Carmon, H. Rokhsari, L. Yang, T. J. Kippenberg, and K. J. Vahala, Phys. Rev. Lett. **94**, 223902 (2005).
[21] A. Schliesser, P. Del'Haye, N. Nooshi, K. J. Vahala, and T. J. Kippenberg, Phys. Rev. Lett. **97**, 243905 (2006).
[22] J. D. Thompson, B. M. Zwickl, A. M. Jayich, F. Marquardt, S. M. Girvin, and J. G. E. Harris, Nature (London) **452**, 72 (2008).
[23] J. K. Viljas and T. T. Heikkilä, Phys. Rev. B **81**, 245404 (2010).
[24] A. Laitinen, M. Oksanen, A. Fay, D. Cox, M. Tomi, P. Virtanen, and P. J. Hakonen, Nano Lett. **14**, 3009 (2014).
[25] T. Stauber, N. M. R. Peres, and A. K. Geim, Phys. Rev. B **78**, 085432 (2008).
[26] R. A. Barton, I. R. Storch, V. P. Adiga, R. Sakakibara, B. R. Cipriany, B. Ilic, S. P. Wang, P. Ong, P. L. McEuen, J. M. Parpia, and H. G. Craighead, Nano Lett. **12**, 4681 (2012).
[27] X. Song, M. Oksanen, J. Li, P. J. Hakonen, and M. A. Sillanpää, Phys. Rev. Lett. **113**, 027404 (2014).
[28] G. Ranjit, C. Montoya, and A. A. Geraci, Phys. Rev. A **91**, 013416 (2015).
[29] B. Renklioglu, B. Tanatar, and M. Ö. Oktel, Phys. Rev. A **93**, 023620 (2016).
[30] P. G. Petrov, S. Machluf, S. Younis, R. Macaluso, T. David, B. Hadad, Y. Japha, M. Keil, E. Joselevich, and R. Folman, Phys. Rev. A **79**, 043403 (2009).
[31] A. Goodsell, T. Ristroph, J. A. Golovchenko, and L. V. Hau, Phys. Rev. Lett. **104**, 133002 (2010).
[32] B. Jetter, J. Märkle1, P. Schneeweiss, M. Gierling, S. Scheel, A. Günther, J. Fortágh, and T. E. Judd, New J. Phys. **15**, 073009 (2013).
[33] P. Schneeweiss, M. Gierling, G. Visanescu, D. P. Kern, T. E. Judd, A. Günther, and J. Fortágh, Nat. Nanotechnol. **7**, 515 (2012).
[34] S. Ribeiro and S. Scheel, Phys. Rev. A **88**, 052521 (2013).
[35] S. Scheel and S. Y. Buhmann, Acta Phys. Slovaca **58**, 675 (2008).

[36] C. T. Weiss, P. V. Mironova, J. Fortágh, W. P. Schleich, and R. Walser, Phys. Rev. A **88**, 043623 (2013).
[37] H. Terças, S. Ribeiro, and J. T. Mendonça, J. Phys. Condens. Matter **27**, 214011 (2015).
[38] Daniel A. Steck, Rubidium 87 D Line Data (revision 2.1.5, 13 January 2015), http://steck.us/alkalidata.
[39] S. Stenholm, Rev. Mod. Phys. **58**, 699 (1986).
[40] T. Blake, A. Kurcz, and A. Beige, J. Mod. Opt. **58**, 1317 (2011).
[41] D. A. R. Dalvit, P. A. Maia Neto, A. Lambrecht, and S. Reynaud, Phys. Rev. Lett. **100**, 040405 (2008).
[42] D. A. R. Dalvit, P. A. Maia Neto, A. Lambrecht, and S. Reynaud, J. Phys. A **41**, 164028 (2008).
[43] F. Reiter and A. S. Sørensen, Phys. Rev. A **85**, 032111 (2012).
[44] X. Hao, S. LiuGang, L. V. XinYou, Y. XiaoXue, and W. Ying, Sci. China Phys. Mech. Astron. **58**, 050302 (2015).
[45] A. L. Gaunt, T. F. Schmidutz, I. Gotlibovych, R. P. Smith, and Z. Hadzibabic, Phys. Rev. Lett. **110**, 200406 (2013).
[46] L. Chomaz, L. Corman, T. Bienaimé, R. Desbuquois, C. Weitenberg, S. Nascimbène, J. Beugnonand, and J. Dalibard, Nat. Commun. **6**, 6162 (2015)
[47] A. D. O'Connell, M. Hofheinz, M. Ansmann, R. C. Bialczak, M. Lenander, E. Lucero, M. Neeley, D. Sank, H. Wang, M. Weides, J. Wenner, J. M. Martinis, and A. N. Cleland, Nature **464**, 697 (2010).
[48] J. D. Teufel, T. Donner, D. Li, J. H. Harlow, M. S. Allman, K. Cicak, A. J. Sirois, J. D. Whittaker, K. W. Lehnert, and R. W. Simmonds, Nature **475**, 359 (2011).
[49] R. W. Peterson, T. P. Purdy, N. S. Kampel, R. W. Andrews, P.-L. Yu, K. W. Lehnert, and C. A. Regal, Phys. Rev. Lett. **116**, 063601 (2016).
[50] M. Antezza, L. P. Pitaevskii, S. Stringari, and V. B. Svetovoy, Phys. Rev. A **77**, 022901 (2008).
[51] M. Antezza, L. P. Pitaevskii, and S. Stringari, Phys. Rev. Lett. **95**, 113202 (2005).
[52] C. Genes, D. Vitali, and P. Tombesi, New J. Phys. **10**, 095009 (2008)
[53] T. Nakajima, P. Lambropoulos, and H. Walther, Phys. Rev. A **56**, 5100 (1997).
[54] Y.-J. Lin, I. Teper, C. Chin, and V. Vuletić, Phys. Rev. Lett. **92**, 050404 (2004).
[55] E. Vetsch, D. Reitz, G. Sagué, R. Schmidt, S. T. Dawkins, and A. Rauschenbeutel, Phys. Rev. Lett. **104**, 203603 (2010).
[56] A. Goban, K. S. Choi, D. J. Alton, D. Ding, C. Lacroûte, M. Pototschnig, T. Thiele, N. P. Stern, and H. J. Kimble, Phys. Rev. Lett. **109**, 033603 (2012).
[57] J. D. Thompson, T. G. Tiecke, N. P. de Leon, J. Feist, A. V. Akimov, M. Gullans, A. S. Zibrov, V. Vuletić, and M. D. Lukin, Science **340**, 1202 (2013).
[58] S. Y. Buhmann and S. Scheel, Phys. Rev. Lett. **100**, 253201 (2008).
[59] M. Chaichian, G. L. Klimchitskaya, V. M. Mostepanenko, and A. Tureanu, Phys. Rev. A **86**, 012515 (2012).
[60] B. E. Sernelius, Phys. Rev. B **85**, 195427 (2012).
[61] D. Drosdoff and L. M. Woods, Phys. Rev. B **82**, 155459 (2010).
[62] I. V. Fialkovsky, V. N. Marachevsky, and D. V. Vassilevich, Phys. Rev. B **84**, 035446 (2011).
[63] I. W. Franck, D. M. Tanenbaum, A. M. van der Zande, and P. L. McEuen, J. Vac. Sci. Technol. B **25**, 2558 (2007).
[64] J. S. Bunch, A. M. van der Zande, S. S. Verbridge, I. W. Frank, D. M. Tanenbaum, J. M. Parpia, H. G. Craighead, and P. L. McEuen, Science **315**, 490 (2007).